# Topography of rods and cones in the retina of the domestic pig

CG Gerke Jr, Y Hao, F Wong

**In a light microscopic study of retinal whole mounts, we quantified the topographical distribution of rod and cone photoreceptors in the domestic pig (*Sus scrofa*). The retina's highest cone density (19 000 to 24 000/mm$^2$) is found above the optic disc, in a broad band slightly below and to the temporal side of the eye's centre. High cone densities averaging 15 000 to 16 000/mm$^2$ extend above this broad band and outwards to the mid-periphery. There is less than a four-fold decrease in cone density between the centre and outer edge of the periphery. Photoreceptor density decreases in proportion to distance from the centre and, conversely, rod frequency increases from an average of 84% in the area of the broad band to 86% to 92% in the far periphery. Taken together, these data indicate that photoreceptor cell distribution is relatively homogeneous in the porcine retina, with the overall ratio of rods to cones at 8:1. In light of the most recent theories to explain human degenerative eye disease, these features of the pig retina make it the most favourable model for therapeutic research into the mechanisms of photoreceptor death in patients with hereditary retinal degeneration.**

*HKMJ 1995;1:302-308*

*Key words: Retina; Rods and cones; Photoreceptors*

## Introduction

Molecular biological techniques have contributed to major breakthroughs in our understanding of hereditary degenerative eye diseases. Among the most significant recent advances is the discovery of specific genetic mutations that can bring on retinitis pigmentosa (RP) and related retinal disorders in which photoreceptor death is a major feature.[1,2] Worldwide, this type of degenerative eye disease afflicts approximately one in every 4000 persons.[3]

Despite our recent genetic discoveries, the ultimate goal of such research remains elusive—we still have little idea of how to design effective treatments for these eye disorders. The major reason for this impasse is the large number of distinct genetic loci now known to be associated with RP.[1,2] In the few genes actually identified, the different types of mutation are many. For example, more than 70 distinct mutations have been identified in the rhodopsin gene of patients suffering autosomal dominant RP.[1,2] The crucial inference here is that the mutations per se are not the direct cause of the observed clinical course of these disorders—some other cellular mechanisms pursuant upon the defective gene's activation ultimately lead to the symptoms.[4,5] Researchers are now hoping to uncover a common factor or pathway that leads to the death of photoreceptors.

To this end, animal models of retinal degeneration have become increasingly important. In three mouse models of RP, for instance, mutations similar to those found in RP patients have been identified, and the shared end result of the mutations in both mice and humans is photoreceptor death. The crucial observation is that the demise of the photoreceptors occurs by apoptosis—a special kind of programmed cell death.[6-8] As a result, scientists have proposed that apoptosis is the final common pathway of photoreceptor death in RP.[6] This hypothesis has proved convincing enough to make apoptosis the major new focus of current therapeutic research.[1] If apoptosis is in fact the common pathway of photoreceptor death induced by a multitude of factors,[6-11] then any therapy that can be devised to prevent photoreceptors from entering into

**Department of Ophthalmology, Duke University School of Medicine, Durham, North Carolina, United States**
CG Gerke Jr, MD
Y Hao, BS
F Wong, PhD
**Correspondence to: Dr F Wong**

apoptosis might prove effective in treating all forms of retinal degeneration.[5]

Another key to designing effective therapy for RP may lie in the pattern of photoreceptor degeneration: over the clinical course of the disease, the rods always die before the cones.[3] With RP-inducing mutations, such as defective rhodopsin, the gene in question is expressed only in rod photoreceptors. Yet some chain of cellular events eventually triggers the death of the cone photoreceptors, which are the vital cells for central vision. Ever since the identification of mutations in the rhodopsin gene, researchers have been nagged by a simple question: why should the cone cells be affected at all?

To help answer this question, researchers may turn to a more appropriate animal model than the mouse: namely, the pig. Anatomically, the porcine eye is remarkably similar to the human eye and—most importantly for the intended studies described here—it is well-endowed with cones.[12] Furthermore, pigs can be genetically engineered to express mutant genes.[13] The creation of transgenic pigs expressing a mutant rhodopsin gene (one resembling the genotype of a form of autosomal dominant RP) is in progress in North Carolina, United States. When this project is complete, we will possess the ideal model in which to pursue the important questions outlined above. Anticipating that the new transgenic pig model will be a strategic focus of vision research in the coming decade, we are presently conducting a series of experiments to provide baseline data for the porcine retina. This report describes the first of the series: a light microscopic study of the topographical distribution of rods and cones in the porcine retina.

## Materials and methods

The eyes of adult (three- to five-year-old) male and female pigs (*Sus scrofa*) were purchased from a local slaughterhouse. Retinal whole mounts were prepared according to the procedure described by Curcio et al[14] with certain modifications. Within one hour of death, the anterior chamber and lens of each eye were removed, and the eyes were placed in Millonig's fixative (4% formaldehyde, 0.155 mol/L sodium monophosphate, 0.105 mol/L sodium hydroxide) for three weeks to three months. Double-edged razors were used to cut each eye into 32 pieces in an approximately radially symmetrical pattern centred at or near the posterior pole. An edge was cut from each piece to help preserve orientation. The retinal portion of each piece was then separated from its underlying pigment epithelium, choroid, and sclera, in 0.1 mol/L sodium phosphate buffer. The retinal fragment was transferred to a 1 mm-thick plastic slide with the photoreceptors facing upward, covered with a 0.2 μm pore-size polycarbonate membrane filter (Millipore, Bedford, Ma, US), flattened, and blotted with bibulous paper. The retina was briefly rinsed in distilled water and the blotting procedure was repeated. Following this, glycerol was applied to the retina, which was covered with a No. 1 coverslip. Figure 1 shows the reconstruction of an entire retina prepared in this manner. The true optical centre was estimated by the midpoints of the total distance along the horizontal and vertical axes of the cut retina.

Photoreceptor layers of whole mounts prepared from porcine eyes were examined with Nomarski differential interference contrast optics, an MTI series 68 video camera (LeMont Scientific, State College, Pa, US), and computerised image analysis with a LeMont OASYS video input image analyser (LeMont Scientific, State College, Pa, US). Images collected with a Nikon OPTIPHOT microscope (Nikon, Garden City,

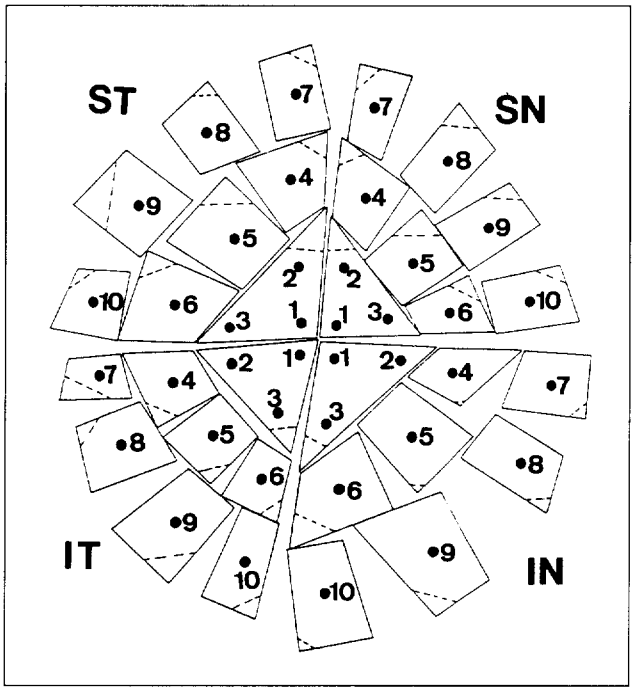


**Fig 1. Diagram illustrating reconstruction of the retina from one of the right eyes examined. ST, SN, IT, and IN denote superior temporal, superior nasal, inferior temporal, and inferior nasal quadrants, respectively. An edge of each piece was removed (dotted lines) to preserve orientation. 400 x Nomarski optical images from regions shown as black dots, marked by numbers and quadrants, were analysed.**

NY, US) at 400 x magnification were calibrated—they appeared at 512 x magnification on the computer monitor. Both rods and cones were counted in each of two to four fields of each retinal region using an interactive counting program. Photoreceptors with half or more of their diameters inside the screen were included in the counts; all others were excluded. Most cell counts were performed at planes of optical dissection passing through the cone ellipsoids (Fig 2b). When it was not possible to clearly visualise both rods and cones at the level of the cone inner segments, separate counts for rods and cones were performed on the same area of the retina at different planes of optical dissection (Figs 2a and 2c). Cell counts for each region of each retina were averaged and the Axum (Trimetrix Inc., Seattle, Wa, US) software package's three-point planar gridding algorithm was used to plot the separate distributions of rods and cones as three-dimensional surface plots. Seven eyes were examined in this fashion. We present data from the three most complete studies: the right and left eyes of one animal and the right eye of a second.

## Results

The major macroscopic feature of the pig retina is an oval optic nerve head. It measures 4.0 to 4.5 mm across and 2.0 to 2.5 mm vertically and is situated in the lower (ventral) temporal portion of the posterior pole.[12] The fine structure of the porcine retina has been detailed elsewhere.[15]

Photoreceptor densities were calculated via light micrographs of flattened whole mounts using Nomarski differential interference contrast optics; this method allows the observer to dissect the retina visually, focusing on a series of different cellular planes of varying depths. We examined two to four fields each of 109 areas from seven eyes (no more than 40 areas in any one eye) and include data from the most complete three.

We concur with Braekevelt's measurements of rod and cone inner and outer segment lengths.[16] The cones, being shorter and stouter than the rods, extend 8 to 10 μm beyond the outer limiting membrane; the inner and outer segments are each approximately 4 to 5 μm long. The longer, more slender rods project through the external limiting membrane for 15 to 20 μm; from 8 to 11 μm of this length is inner segment. The retinal whole mount shown in Fig 2 demonstrates a typical view of the mid-peripheral region at 400 x magnification. An optical dissection of the inner and outer segments of the pig's upward-facing photoreceptor layer is shown

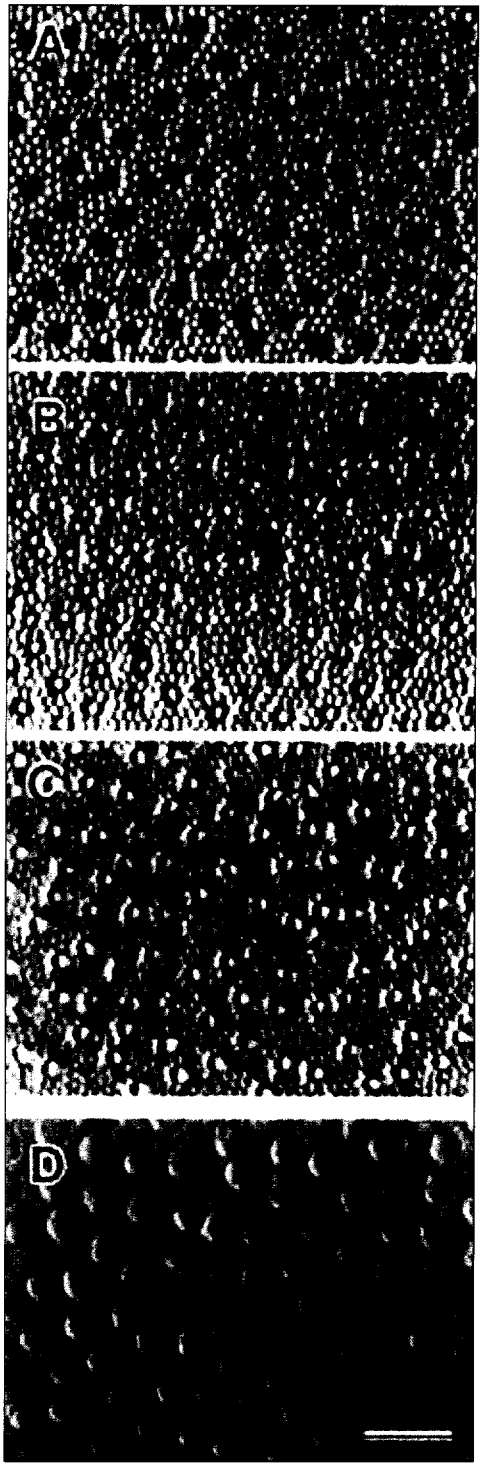


**Fig 2. 400 x Nomarski optical dissection of photoreceptor inner and outer segments. 2a. Most superficially, only the inner and outer segments of rods can be seen. 2b. As the plane of focus is moved inward, the bright cone outer segments can be visualised. 2c. At a deeper level still, the diameters of the cone outer segments have increased, and the rods are packed more tightly together. 2d. At the deepest plane of optical dissection, only the large cone inner segments can be seen.**
**Scale shows 20 μm.**

in Figs 2a to 2d. Photoreceptor inner and outer segments appear as circular profiles of different diameters and brightness. In the deepest plane focus (Fig 2d) only the large cone ellipsoids can be seen distinctly. The rod myoids are situated at the level of the cone ellipsoids;[15] this is consistent with Miller and Snyder's two-tiered model for the retina.[17] Photoreceptor myoids tend to be less clearly outlined than ellipsoids, especially when spatial constraints demand tight packing. As the plane of focus is moved superficially (Figs 2c and 2b), the diameters of the cone profiles decrease and the rod inner segments become more distinct. At the most superficial plane of focus (Fig 2a), the shorter cones cannot be seen; holes in the matrix of rod inner and outer segments mark the cone locations. Figure 3 demonstrates the range of photoreceptor densities found in one eye. The inner segments of photoreceptors (especially cones) in the central retina are narrower than those found in the periphery; this permits greater photoreceptor densities in central areas.

We have analysed the rod and cone density averages and standard deviations of each of the seven eyes studied. These densities were not corrected for the minimal linear expansion (<4%) which typically occurs during the preparation of whole mounts.[14] The overall distribution of photoreceptors in these seven eyes was quite similar.

Because of clear differences in retinal areas, cut-out patterns, and portions sampled from each cut piece, the data points of the three eyes do not precisely correspond. We therefore grouped the cut regions into 10 zones of various sizes based on the generalised pattern of photoreceptor distribution in the three eyes (Fig 4). Values for each zone were obtained from approximately corresponding regions of each eye and each eye was given equal weight when determining the average densities (Table 1) for the zone, irrespective of the number of cut regions sampled from the eye.

Figure 4 shows a 2.5 x 15.0 mm visual streak of high cone density situated parallel to the horizontal axis; its centre was situated a small distance below and temporal to the centre, and above the optic disc. This finding was consistent with previous speculation, based on the arrangement of the pig's vascular tree, as to the existence of an area centralis extending from the temporal side of the papilla to the posterior pole.[12] In addition, we discovered a second, smaller area of high cone density, approximately 2 mm in diameter, in the nasal mid-periphery. High cone densities extended above and to the temporal side, from the visual streak to the mid-periphery. As shown in Table 1, all

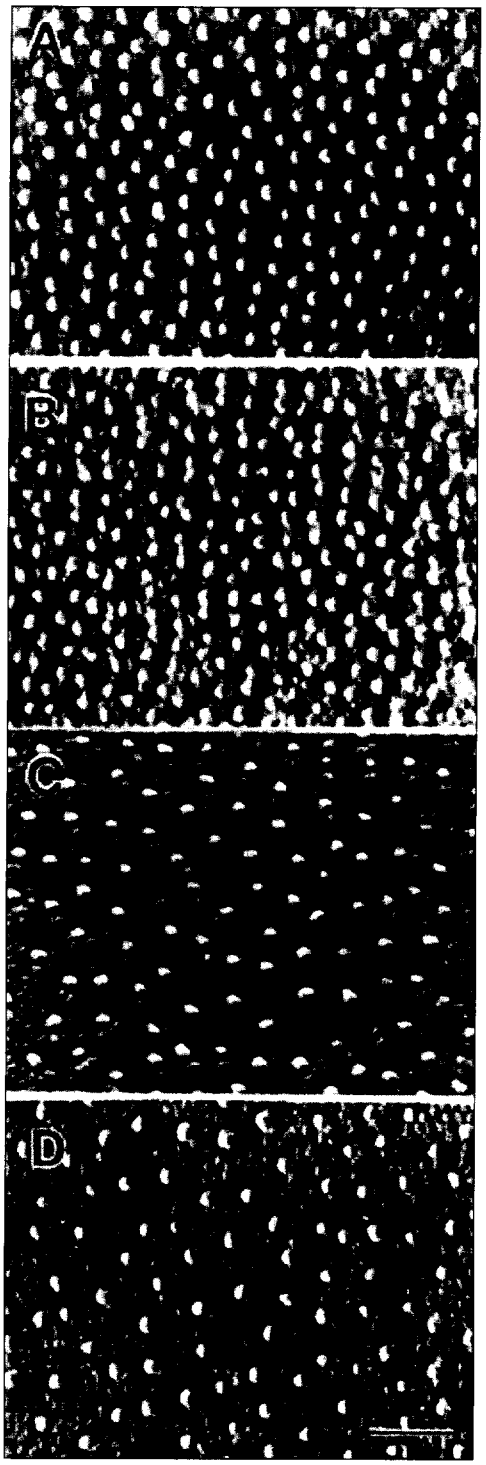


**Fig 3a. Visual streak. 3b. Second area of highest cone density. 3c. Inferior temporal mid-periphery. 3d. Inferior nasal far periphery. The circular profiles of the rods are smaller and darker than those of the cones.**
**Scale shows 20 μm.**

superior and central regions of the pig's retina had higher cone densities than any portion of the human retina outside the macula. The pig's lower far periphery had cone densities equivalent to those found in the

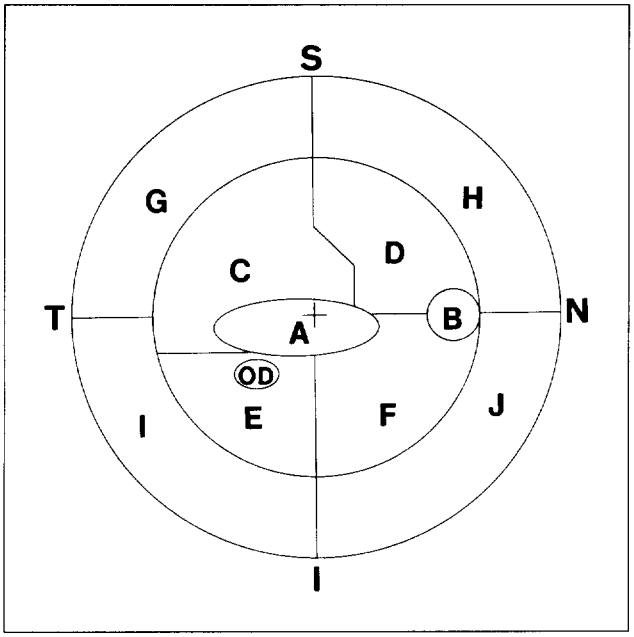


**Fig 4. S, I, T and N indicate the superior, inferior, temporal, and nasal directions, respectively, from the centre. OD = optic disc; + = centre. A represents the first area of high cone density; B shows a second, smaller area of high cone density which is located in the mid-periphery. Photoreceptor densities of each zone are given in Table 1.**

human near- and mid-periphery. Whereas the human rod:cone ratio reaches a peak of 20 to 30:1 in the mid-periphery,[18] the rod:cone ratio of the pig reached a maximum of only 10 to 15:1 in the far periphery of its inferior retina. Rods appeared in greatest numbers in the pig's temporal retina and in the two areas of highest cone density. Their numbers declined with increasing eccentricity; this decline was greater above and on the nasal side than below and on the temporal side.

The finding of a second area of high cone density was unexpected—it has never been demonstrated in any non-avian vertebrate. In every porcine eye examined, the cone density first decreased, then increased along a portion of the nasal mid-periphery adjacent to the horizontal axis. The existence of these two areas is graphically demonstrated by the distribution of cones in one eye illustrated as a three-dimensional surface plot in Fig 5. The surface contour of the cone distribution of this eye revealed high cone densities extending above and temporally from the visual streak. The overall cone density of the superior retina was higher than that of the inferior retina. Although Fig 5 depicts a rectangular representation of the retina, this is an artefact due to the method of generating surface plots. The portion which represents cone density is the largest cylindrical shape with its base in the x-y plane. Figure 5 is presented only as a visual aid for interpreting Fig 4 and Table 1. Nevertheless, the separation into two

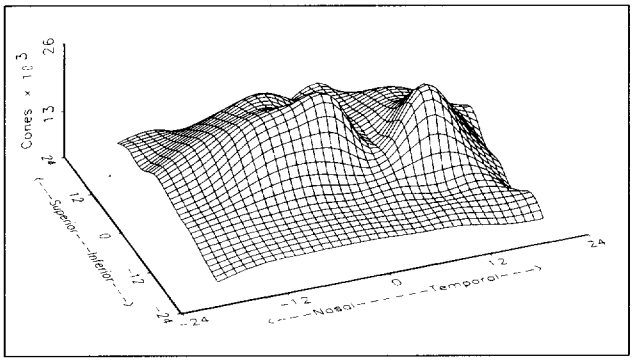


**Fig 5. X- and Y-axes display millimetres distance from the optical centre; thousands of cones per mm² are plotted on the Z-axis. The Z-axis origin has been set to 4000 cones per mm² in order to enhance the contrast between regions.**

**Table 1. Photoreceptor densities (per mm²) and ratios of rods to cones for the 10 zones depicted in Fig. 4. 1. Mean numbers of photoreceptors per mm² ± one RMS deviation from the mean of three porcine retinas for the 10 zones depicted in Fig 4.**

| Zone | Cones | Rods | Rods:cones |
|---|---|---|---|
| A | 21 498 ± 2165 | 113 093 ± 793 | 5.3:1 |
| B | 18 650 ± 4807 | 98 501 ± 7121 | 5.3:1 |
| C | 15 753 ± 241 | 102 819 ± 9573 | 6.5:1 |
| D | 12 904 ± 132 | 84 468 ± 9573 | 6.5:1 |
| E | 10 713 ± 798 | 110 839 ± 2303 | 10.3:1 |
| F | 10 084 ± 1115 | 97 561 ± 5789 | 9.7:1 |
| G | 10 841 ± 352 | 76 560 ± 6662 | 7.1:1 |
| H | 10 539 ± 1896 | 65 850 ± 510 | 6.2:1 |
| I | 7238 ± 754 | 85 450 ± 11993 | 11.8:1 |
| J | 6773 ± 681 | 81 025 ± 5484 | 12.0:1 |

areas of high cone densities rather than one continuous area was clearly demonstrated. In two of the eyes, we repeat-sampled and counted photoreceptors in areas which supported the two-area hypothesis (the nasal edges of the retinal sections where the decrease had been found). In these two eyes, the average photoreceptor density in the region of the second area was more than two standard deviations from the average photoreceptor density of at least one intervening region between it and the first area.

## Discussion

Previous investigators have offered a variety of estimates of the overall ratio of rods to cones in the porcine retina; these include 7:1,[15] 93:7 (approximately 13:1),[17] and 25 to 30:1.[16] The oldest data are the most accurate; we found that the average ratio of rods to cones in the entire porcine retina was approximately 8:1. The 7:1 ratio observed by Beauchemin can be seen in almost every quadrant.[15] The ratio of 13:1 was seen in fields in the inferior far periphery.[17] We have not observed a ratio of rods to cones greater than 17:1 in any area, even near the ora terminalis.

The visual streak below the level of the centre is a retinal characteristic that the pig shares with many other animals. The ganglion cell layers of pigs, sheep, oxen, and horses show a streak of small ganglion cells along the horizontal axis below the optical centre. Likewise, the vascular arrangement of the fox and the rabbit is such that their visual streaks are also likely to lie below the posterior pole.[12] This pattern is even conserved in the photoreceptors and ganglion cells of at least one amphibian—the toad (*Bufo marinus*).[19]

The major retinal vessels in the pig avoid crossing almost the entire nasal-temporal meridian (both nasal and temporal to the optic disc). Only the superior retinal artery and the superior retinal vein cross this region at all, and then almost at right angles. This has been demonstrated both by scanning electron microscopic imaging of resin-infused retina[20] and by fluorescein angiography.[21] This arrangement implies the possibility of a temporal visual streak[12] and could support a second macula-like region nasal to the pig's temporal area of high cone density.

In general, the average ratio of rods to cones in the porcine retina is 8:1, and this ratio is fairly homogeneous across the retina. The relative abundance of cones makes the porcine eye ideal for future vision research, insofar as investigators are now focusing on the interrelations of rods and cones in programmed cell death as brought on by degenerative eye diseases.[22] The pig should prove to be the most important model for researchers who seek to evaluate the various pathological processes of retinal diseases with a view toward therapeutic intervention—by gene transfection, cell transplant, or intravitreal injection of growth factors.

## Acknowledgments

The authors acknowledge the assistance of Ms AE Gaitan for the photography and Dr MA Hipsky for editing this paper. This work was supported in part by a National Eye Institute grant EY09047 and a grant from the Foundation Fighting Blindness of Baltimore, Maryland, US. Dr Wong is a Senior Scientific Investigator of Research to Prevent Blindness Inc., of New York, US.

## References

1. Bird AC. Retinal photoreceptor dystrophies LI: Edward Jackson Memorial Lecture. Am J Ophthalmol 1995;119:543-62.
2. Dryja TP, Berson EL. Retinitis pigmentosa and allied diseases: implications of genetic heterogeneity. Invest Ophthalmol Vis Sci 1995;36:1197-200.
3. Berson EL. Retinitis pigmentosa: the Friedenwald lecture. Invest Ophthalmol Vis Sci 1993;34:1659-76.
4. Wong F. Visual pigments, blue cone monochromasy, and retinitis pigmentosa. Arch Ophthalmol 1990;108:935-6.
5. Wong F. How shall research in the treatment of retinitis pigmentosa proceed? Arch Ophthalmol 1993;111:754-6.
6. Chang GQ, Hao Y, Wong F. Apoptosis: final common pathway of photoreceptor death in *rd*, *rds*, and rhodopsin mutant mice. Neuron 1993;11:595-605.
7. Lolley RN, Rong H, Craft CM. Linkage of photoreceptor degeneration by apoptosis with the inherited defect in phototransduction. Invest Ophthalmol Vis Sci 1994;35:358-62.
8. Portera-Cailliau C, Sung CH, Nathans J, Adler R. Apoptotic photoreceptor cell death in mouse models of retinitis pigmentosa. Proc Natl Acad Sci USA 1994;91:974-8.
9. Tso MO, Zhang C, Abler AS, et al. Apoptosis leads to photoreceptor degeneration in inherited retinal dystrophy of RCS rats. Invest Ophthalmol Vis Sci 1994;35:2693-6.
10. Cook B, Lewis GP, Fisher SK, Adler R. Apoptotic photoreceptor degeneration in experimental retinal detachment. Invest Ophthalmol Vis Sci 1995;36:990-6.
11. Chang CJ, Lai WW, Edward DP, Tso MO. Apoptotic photoreceptor cell death after traumatic retinal detachment in humans. Arch Ophthalmol 1995;113:880-6.
12. Prince JH, Diesem CD, Eglitis I, Ruskell GL. editors. The pig. In: Anatomy and histology of the eye and orbit in domestic animals. Springfield, Ill: Charles C Thomas, 1960: 210-33.
13. Pursel VG, Pinkert CA, Miller KF, et al. Genetic engineering of livestock. Science 1989;244:1281-8.
14. Curcio CA, Packer O, Kalina RE. A whole mount method for sequential analysis of photoreceptor and ganglion cell topography in a single retina. Vis Res 1987;27:9-15.

15. Beauchemin ML. The fine structure of the pig's retina. Graefe's Arch Clin Exp Ophthalmol 1974;190:27-45.
16. Braekevelt CR. Fine structure of the retinal rods and cones in the domestic pig. Graefe's Arch Clin Exp Ophthalmol 1983;220:273-8.
17. Miller WH, Snyder AW. The tiered vertebrate retina. Vis Res 1977;17:239-55.
18. Curcio CA, Sloan KR, Kalina RE, Hendrickson AE. Human photoreceptor topography. J Comp Neurol 1990;292:497-523.
19. Zhang Y, Straznicky C. The morphology and distribution of photoreceptors in the retina of *Bufo marinus*. Anat Embryol 1991;183:97-104.
20. Simoens P, de Schaepdrijver L, Lauwers H. Morphologic and clinical study of the retinal circulation in the miniature pig. A: morphology of the retinal microvasculature. Exp Eye Res 1992;54:965-73.
21. de Schaepdrijver L, Simoens P, Pollet L, Lauwers H, de Laey J. Morphologic and clinical study of the retinal circulation in the miniature pig. B: fluorescein angiography of the retina. Exp Eye Res 1992;54:975-85.
22. Huang PC, Gaitan AE, Hao Y, Petters RM, Wong F. Cellular interactions implicated in the mechanism of photoreceptor degeneration in transgenic mice expressing a mutant rhodopsin gene. Proc Natl Acad Sci USA 1993;90:8484-8.